View metadata, citation and similar papers at core.ac.uk

brought to you by CORE

provided by Elsevier - Publisher Connector

Physics Letters B 710 (2012) 454–459

Contents lists available at SciVerse ScienceDirect

Physics Letters B

www.elsevier.com/locate/physletb

The constrained NMSSM and Higgs near 125 GeV

John F. Gunion [a], Yun Jiang [a], Sabine Kraml [b,*]

[a] Department of Physics, University of California, Davis, CA 95616, USA

[b] Laboratoire de Physique Subatomique et de Cosmologie, UJF Grenoble 1, CNRS/IN2P3, INPG, 53 Avenue des Martyrs, F-38026 Grenoble, France

ARTICLE INFO

Article history:
Received 25 January 2012
Received in revised form 3 March 2012
Accepted 13 March 2012
Available online 16 March 2012
Editor: G.F. Giudice

ABSTRACT

We assess the extent to which various constrained versions of the NMSSM are able to describe the recent hints of a Higgs signal at the LHC corresponding to a Higgs mass in the range 123–128 GeV.

© 2012 Elsevier B.V. All rights reserved.

The Large Hadron Collider (LHC) data from the ATLAS [1] and CMS [2] Collaborations suggests the possibility of a fairly Standard Model (SM) like Higgs boson with mass of order 123–128 GeV. In particular, promising hints appear of a narrow excess over background in the $\gamma\gamma$ and $ZZ \to 4\ell$ final states with strong supporting evidence from the $WW \to \ell\nu\ell\nu$ mode. While the ATLAS and CMS results suggest that the $\gamma\gamma$ rate may be somewhat enhanced with respect to the SM expectation, this is by at most one standard-deviation (1σ).

In this Letter, we explore the ability or lack thereof of three constrained versions of the Next-to-Minimal Supersymmetric Standard Model (NMSSM) to describe these observations while remaining consistent with all relevant constraints, including those from LEP and TEVATRON searches, B-physics, the muon anomalous magnetic moment, $a_\mu \equiv (g-2)_\mu/2$, and the relic density of dark matter, Ωh^2.

The possibility of describing the LHC observations in the context of the MSSM has been explored in numerous papers, including [3–11]. A general conclusion seems to be that if all the constraints noted above, including a_μ and Ωh^2, are imposed rigorously, then the MSSM—especially a constrained version such as the CMSSM—is hard pressed to yield a fairly SM-like light Higgs boson at 125 GeV. This is somewhat alleviated when the a_μ constraint is dropped [3,7]. Overall, however, large mixing and large SUSY masses are needed to achieve $m_h \sim 125$ GeV. There has also been some exploration in the context of the NMSSM [12,13,11], showing that for completely general parameters there is less tension between a light Higgs with mass ~ 125 GeV and a lighter SUSY mass spectrum. The study presented here will be done in the context of several constrained versions of the NMSSM with universal or semi-universal GUT scale boundary conditions. Results for a very constrained version of the NMSSM, termed the cNMSSM, appear in [14,15,4]—we discuss comparisons later in the Letter.

The three models which we discuss here are defined in terms of grand-unification (GUT) scale parameters as follows: **I**) a version of the constrained NMSSM (CNMSSM) in which we adopt universal m_0, $m_{1/2}$, $A_0 = A_{t,b,\tau}$ values but require $A_\lambda = A_\kappa = 0$, as motivated by the $U(1)_R$ symmetry limit of the NMSSM; **II**) the non-universal Higgs mass (NUHM) relaxation of model **I** in which m_{H_u} and m_{H_d} are chosen independently of m_0, but still with $A_\lambda = A_\kappa = 0$; and **III**) universal m_0, $m_{1/2}$, A_0 with NUHM relaxation and general A_λ and A_κ.

We use NMSSMTools-3.0.2 [16–18] for the numerical analysis, performing extensive scans over the parameter spaces of the models considered. The precise constraints imposed are the following. Our 'basic constraints' will be to require that an NMSSM parameter choice be such as to give a proper RGE solution, have no Landau pole, have a neutralino LSP and obey Higgs and SUSY mass limits as implemented in NMSSMTools-3.0.2 (Higgs mass limits are from LEP, TEVATRON, and early LHC data; SUSY mass limits are essentially from LEP). Regarding B physics, the constraints considered are those on $\mathrm{BR}(B_s \to X_s\gamma)$, ΔM_s, ΔM_d, $\mathrm{BR}(B_s \to \mu^+\mu^-)$, $\mathrm{BR}(B^+ \to \tau^+\nu_\tau)$ and $\mathrm{BR}(B \to X_s\mu^+\mu^-)$ at 2σ as encoded in NMSSMTools-3.0.2, except that we updated the bound on the radiative B_s decay to $3.04 < \mathrm{BR}(B_s \to X_s\gamma) \times 10^4 < 4.06$; theoretical uncertainties in B-physics observables are taken into account as implemented in NMSSMTools-3.0.2. These combined constraints we term the 'B-physics constraints'. Regarding a_μ, we require that the extra NMSSM contribution, δa_μ, falls into the window defined in NMSSMTools of $8.77 \times 10^{-10} < \delta a_\mu < 4.61 \times 10^{-9}$ expanded to $5.77 \times 10^{-10} < \delta a_\mu < 4.91 \times 10^{-9}$ after allowing for a 1σ theoretical error in the NMSSM calculation of $\pm 3 \times 10^{-10}$. In fact, points

* Corresponding author.
E-mail address: sabine.kraml@lpsc.in2p3.fr (S. Kraml).

0370-2693/$ – see front matter © 2012 Elsevier B.V. All rights reserved.
http://dx.doi.org/10.1016/j.physletb.2012.03.027

that fail to fall into the above δa_μ window always do so by virtue of δa_μ being too small. For Ωh^2, we declare that the relic density is consistent with WMAP data provided $0.094 < \Omega h^2 < 0.136$, which is the 'WMAP window' defined in NMSSMTools-3.0.2 after including theoretical and experimental systematic uncertainties. We will also consider the implications of relaxing this constraint to simply $\Omega h^2 < 0.136$ so as to allow for scenarios in which the relic density arises at least in part from some other source. A "perfect" point will be one for which all constraints are satisfied including requiring that δa_μ is in the above defined window and Ωh^2 is in the WMAP window.

We find that only in models **II** and **III** is it possible for a "perfect" point to have a light scalar Higgs in the mass range 123–128 GeV as consistent with the hints from the recent LHC Higgs searches. The largest m_{h_1} achieved for perfect points is about 125 GeV. However, relaxing the a_μ constraint vastly increases the number of accepted points and it is possible to have $m_{h_1} \gtrsim 126$ GeV in both models **II** and **III** even if δa_μ is just slightly outside (below) the allowed window. Comparing with [3], the tension between obtaining an ideal or nearly ideal δa_μ while predicting a SM-like light Higgs near 125 GeV appears to be somewhat less in NUHM variants of the NMSSM than in those of the MSSM.

In the plots shown in the following, the coding for the plotted points is as follows:

- grey squares pass the 'basic' constraints but fail B-physics constraints (such points are rare);
- green squares pass the basic constraints *and* satisfy B-physics constraints;
- blue pluses (+) observe B-physics constraints as above and in addition have $\Omega h^2 < 0.136$, thereby allowing for other contributions to the dark matter density (a fraction of order 20% of these points have $0.094 < \Omega h^2 < 0.136$) but they do not necessarily have acceptable δa_μ;
- magenta crosses (×) have satisfactory δa_μ as well as satisfying B-physics constraints, but arbitrary Ωh^2;
- golden triangle points pass all the same constraints as the magenta points and in addition have $\Omega h^2 < 0.136$;
- open black/grey[1] triangles are perfect, completely allowed points in the sense that they pass all the constraints listed earlier, including $5.77 \times 10^{-10} < \delta a_\mu < 4.91 \times 10^{-9}$ and $0.094 < \Omega h^2 < 0.136$;
- open white diamonds are points with $m_{h_1} \geqslant 123$ GeV that pass basic constraints, B-physics constraints and predict $0.094 < \Omega h^2 < 0.136$ but have $4.27 \times 10^{-10} < \delta a_\mu < 5.77 \times 10^{-10}$, that is we allow an excursion of half the 1σ theoretical systematic uncertainty below the earlier defined window. We will call these "almost perfect" points.

The only Higgs production mechanism relevant for current LHC data is gluon–gluon to Higgs. For our plots it will thus be useful to employ the ratio of the gg induced Higgs cross section times the Higgs branching ratio to a given final state, X, relative to the corresponding value for the SM Higgs boson:

$$R^{h_i}(X) \equiv \frac{\Gamma(gg \to h_i)\,\mathrm{BR}(h_i \to X)}{\Gamma(gg \to h_{\mathrm{SM}})\,\mathrm{BR}(h_{\mathrm{SM}} \to X)}, \tag{1}$$

where h_i is the ith NMSSM scalar Higgs, and h_{SM} is the SM Higgs boson. The ratio is computed in a self-consistent manner (that is, treating radiative corrections for the SM Higgs boson in the same manner as for the NMSSM Higgs bosons) using an appropriate additional routine for the SM Higgs added to the NMHDECAY component of the NMSSMTools package. To compute the SM denominator, we proceed as follows.[2] NMHDECAY computes couplings for each h_i defined by $C_Y^{h_i} \equiv g_{h_i Y}/g_{h_{\mathrm{SM}} Y}$, where $Y = gg, VV, b\bar{b}, \tau^+\tau^-, \gamma\gamma, \ldots$, as well as $\Gamma_{\mathrm{tot}}^{h_i}$ and $\mathrm{BR}(h_i \to Y)$ for all Y. From these results we obtain the partial widths $\Gamma^{h_i}(Y) = \Gamma_{\mathrm{tot}}^{h_i}\,\mathrm{BR}(h_i \to Y)$. We next compute $\Gamma^{h_{\mathrm{SM}}}(Y) = \Gamma^{h_i}(Y)/[C_Y^{h_i}]^2$ and $\Gamma_{\mathrm{tot}}^{h_{\mathrm{SM}}} = \sum_Y \Gamma^{h_{\mathrm{SM}}}(Y)$ and thence $\mathrm{BR}(h_{\mathrm{SM}} \to Y) = \Gamma^{h_{\mathrm{SM}}}(Y)/\Gamma_{\mathrm{tot}}^{h_{\mathrm{SM}}}$. We then have all the information needed to compute R^{h_i} for some given final state X.

We begin by presenting the crucial plots of Fig. 1 in which we show $R^{h_1}(\gamma\gamma)$ as a function of m_{h_1} for cases **I**, **II** and **III**. Only in cases **II** and **III** do we find points that pass all constraints (the open black triangles) with $m_{h_1} \sim 124$–125 GeV. These typically have $R^{h_1}(\gamma\gamma)$ of order 0.98. Somewhat surprisingly, such points were more easily found by our scanning procedure in case **II** than in case **III**. Many additional points with $m_{h_1} \sim 125$ GeV emerge if we relax only slightly the δa_μ constraint. The white diamonds show points for cases for which $4.27 \times 10^{-10} < \delta a_\mu < 5.77 \times 10^{-10}$ having $m_{h_1} \geqslant 123$ GeV. As can be seen in more detail from the sample point tables presented later, the parameter choices that give the largest m_{h_1} values are ones for which the h_1 is really very SM-like in terms of its couplings and branching ratios. Our scans did not find parameter choices for which $R^{h_1}(\gamma\gamma)$ was significantly larger than 1 for $m_{h_1} = 123$–128 GeV, as hinted at by the ATLAS data.

As regards h_2, if we require $m_{h_2} \in [110\text{–}150]$ GeV then we find points that pass the basic constraints and the B-physics constraints, but none that pass the further constraints. So, it appears that within these models it is the h_1 that must be identified with the Higgs observed at the LHC. In contrast, if parameters are chosen at the SUSY scale without regard to GUT-scale unification, it is possible to find scenarios in which $m_{h_2} \approx 125$ GeV and, moreover, $R^{h_2}(\gamma\gamma) > 1$ [13].

In passing, we note that should the Higgs hints disappear and a low-mass SM-like Higgs be excluded then it is of interest to know if $\mathrm{BR}(h_1 \to a_1 a_1)$ can be large for m_{h_1} in the $\lesssim 130$ GeV range. It turns out that, although large $\mathrm{BR}(h_1 \to a_1 a_1)$ is possible while satisfying basic and B-physics constraints, once additional constraints are imposed, $\mathrm{BR}(h_1 \to a_1 a_1) \lesssim 0.2$ for all three model cases being considered. Small $\mathrm{BR}(h_1 \to a_1 a_1)$ is expected [20] (see also [21]) when the a_1 is very singlet, as is the case in our scenarios once all constraints are imposed. So, in these models a light Higgs has nowhere to hide.

The points in the scatter plots were primarily obtained through random scans over the parameter spaces of the three models considered. In addition, we performed Markov Chain Monte Carlo (MCMC) scans to zero in better on points with $m_{h_1} \sim 125$ GeV that observe all constraints. For this purpose, we defined a $\chi^2(m_{h_1}) = (m_{h_1} - 125)^2/(1.5)^2$. The B-physics constraints were also implemented using a χ^2 approach with the 1σ errors from theory and experiment (as implemented in NMSSMTools) combined in quadrature. The global likelihood was then computed as $L_{\mathrm{tot}} = \prod_i L_i$ with $L_i = e^{-\chi_i^2/2}$ for two-sided constraints and $L_i = 1/(1 + e^{(x_i - x_i^{\mathrm{exp}})}/(0.01 x_i^{\mathrm{exp}}))$ when x_i^{exp} is a 95% CL upper limit. The a_μ and Ωh^2 constraints were either implemented a-posteriori using the 2σ window approach of NMSSMTools, or also included in

[1] For perfect points, we will use black triangles if $m_{h_1} \geqslant 123$ GeV and grey triangles if $m_{h_1} < 123$ GeV in plots where m_{h_1} does not label the x axis.

[2] Ideally, the same radiative corrections would be present in NMHDECAY as are present in HDECAY [19] and we could then employ HDECAY results for the SM Higgs denominator. But, this is not the case at present, with HDECAY yielding, e.g., larger gg production rates. However, we note that since we compute the ratios of NMSSM rates to SM rates using the C_Y couplings, as discussed below, the computed ratios will be quite insensitive to the precise radiative corrections employed.

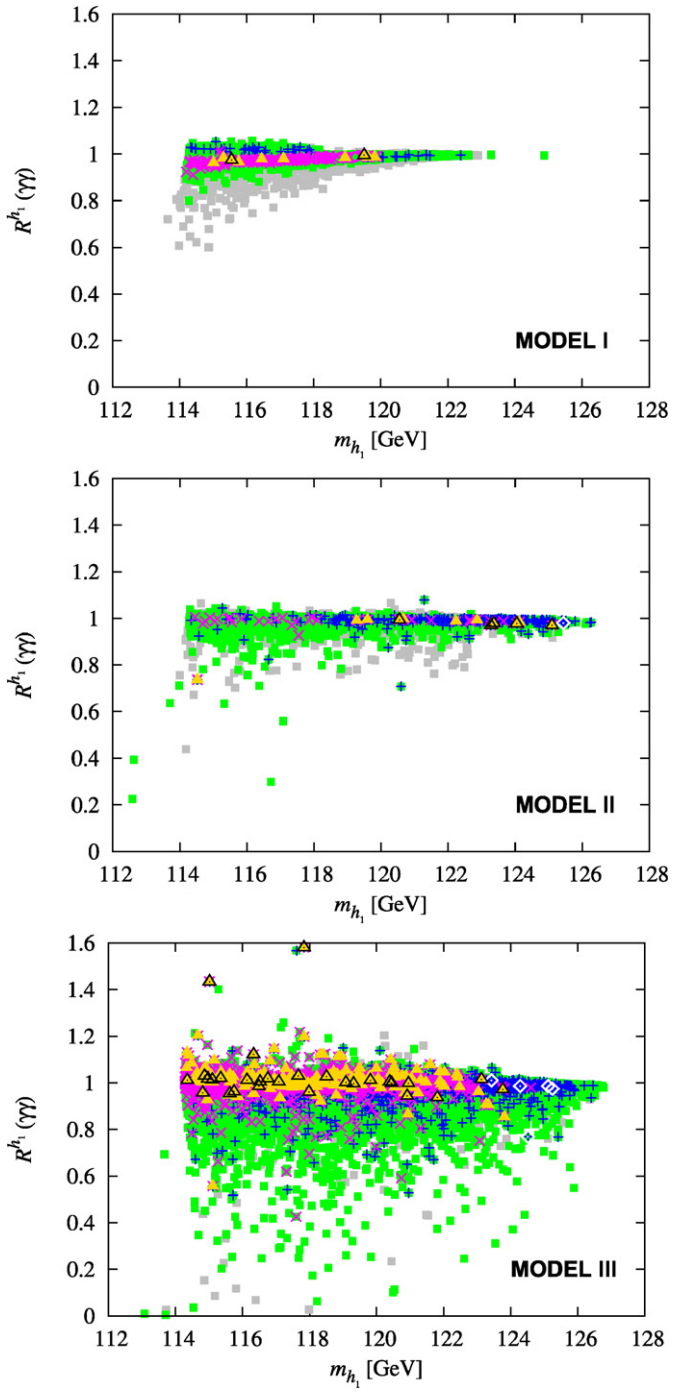

Fig. 1. Scatter plots of $R^{h_1}(\gamma\gamma)$ versus m_{h_1} for boundary condition cases **I**, **II** and **III**. See text for symbol/color notations. (For interpretation of the references to color in this figure, the reader is referred to the web version of this Letter.)

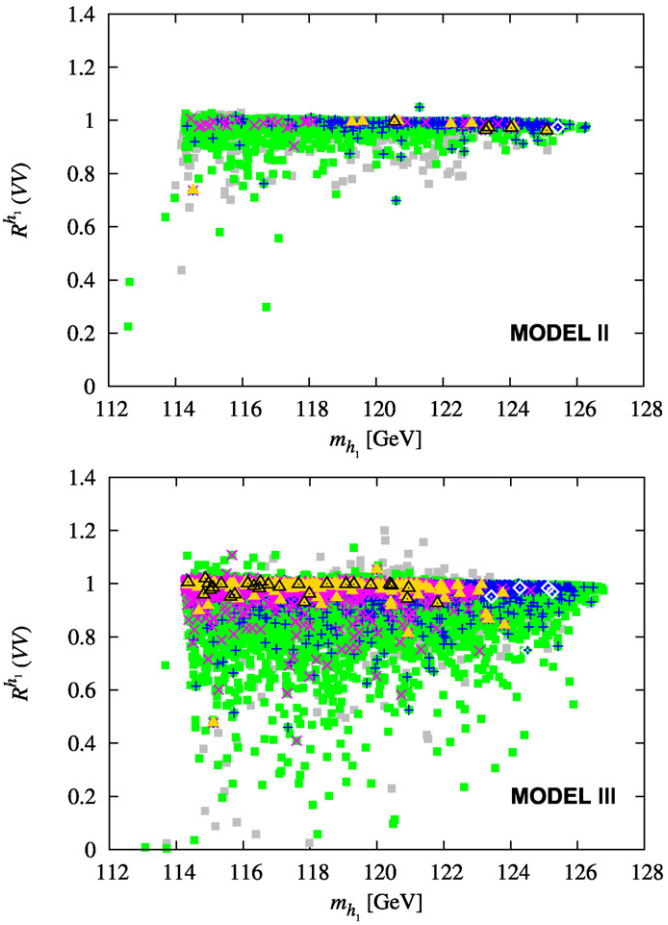

Fig. 2. Scatter plots of $R^{h_1}(VV = ZZ, WW)$ versus m_{h_1} for models **II** and **III**. See text for symbol/color notations. (For interpretation of the references to color in this figure, the reader is referred to the web version of this Letter.)

the global likelihood. Since CMSSM-like boundary conditions with $A_\lambda = A_\kappa = 0$ did not generate points anywhere near the interesting region, we have only performed this kind of scan for cases **II** and **III**. This allowed us to find additional "perfect" and "almost perfect" points for models **II** and **III** with $m_{h_1} \gtrsim 123$ GeV.

We next illustrate in Fig. 2 $R^{h_1}(VV)$ (the ratio being the same for $VV = WW$ and $VV = ZZ$) for boundary condition cases **II** and **III**. As for the $\gamma\gamma$ final state, for $m_{h_1} \gtrsim 123$ GeV the predicted rates in the VV channels are very nearly SM-like. Overall, it is clear that, for the GUT scale boundary conditions considered here, one finds that for parameter choices yielding consistency with all constraints and yielding m_{h_1} close to 125 GeV, the h_1 will be very SM-like. If future data confirms a $\gamma\gamma$ rate in excess of the SM prediction, then it will be necessary to go beyond the constrained versions of the NMSSM considered here (cf. [13]). And, certainly it is very difficult within the constrained models considered here to obtain a SM-like Higgs with mass much above 126 GeV for parameter choices such that all constraints, including δa_μ and Ωh^2, are satisfied.

Should a later LHC data set prove consistent with a rather SM-like Higgs in the vicinity of $m_{h_1} \sim 125$ GeV (rather than one with an enhanced $\gamma\gamma$ rate), it will be of interest to know the nature of the parameter choices that yield the perfect, black triangle and almost perfect white diamond points with $m_{h_1} \sim 125$ GeV and what the other experimental signatures of these points are. We therefore present a brief summary of the most interesting features. First, one must ask if such points are consistent with current LHC limits on SUSY particles, in particular squarks and gluinos. To this end, Fig. 3 shows the distribution of squark and gluino masses for the various kinds of points for models **II** and **III**. Interestingly, all the perfect, black triangle and almost perfect, white diamond points with $m_{h_1} \gtrsim 123$ GeV have squark and gluino masses above 1 TeV and thus have not yet been probed by current LHC results. (Note that since we are considering models with universal m_0 and $m_{1/2}$ for squarks and gauginos, analyses in the context of the CMSSM apply.) It is quite intriguing that the regions of parameter space that are consistent with a Higgs of mass close to

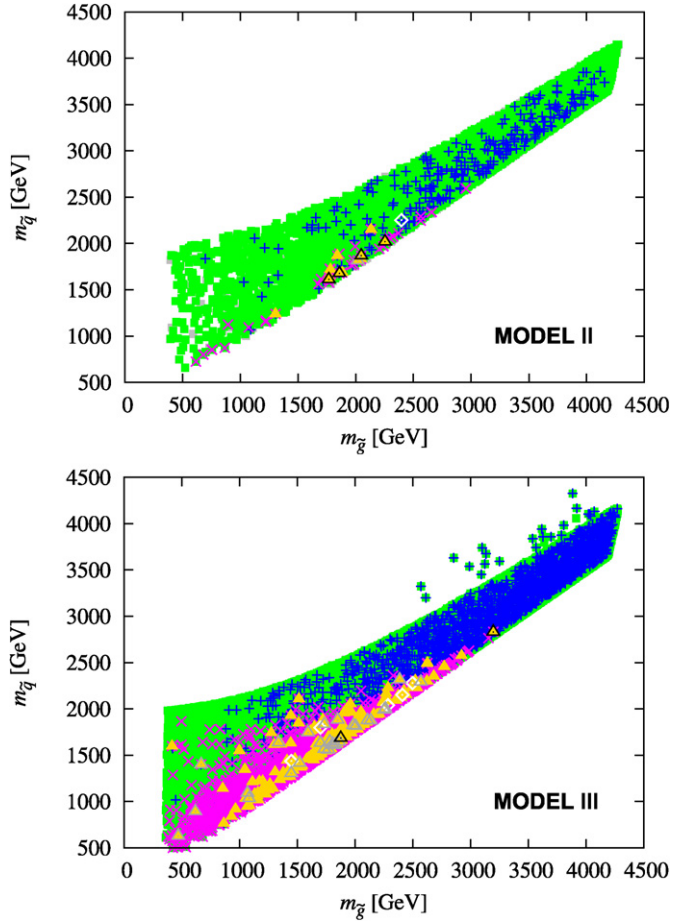

Fig. 3. Scatter plots of squark versus gluino masses for models **II** and **III**. Here we use black (grey) open triangles for perfect points with $m_{h_1} \geqslant 123$ GeV ($m_{h_1} < 123$ GeV). See text for remaining symbol/color notations. (For interpretation of the references to color in this figure, the reader is referred to the web version of this Letter.)

125 GeV automatically evade the current limits from LHC SUSY searches.

In order to further detail the parameters and some relevant features of perfect and almost perfect points we present in Tables 1–4 seven exemplary points with $m_{h_1} \gtrsim 124$ GeV from models **II** and **III**. Some useful observations include the following:

- Because of the way we initiated our model **III** MCMC scans, restricting $|A_{\lambda,\kappa}| \leqslant 1$ TeV, most of the tabulated model **III** points have quite modest A_λ and A_κ. However, a completely random scan finds almost perfect points with quite large A_λ and A_κ values as exemplified by tabulated point #7. The fact that the general scan over A_λ and A_κ did not find any perfect points with $m_{h_1} \gtrsim 124$ GeV, whereas such points were fairly quickly found using the MCMC technique, suggests that such points are quite fine-tuned in the general scan sense. See Table 1 for specifics.
- In Table 2, we display various details regarding the Higgs bosons for each of our exemplary points. As already noted, for the perfect and almost perfect points the h_1 is very SM-like when $m_{h_1} \gtrsim 123$ GeV. To quantify how well the LHC Higgs data is described for each of our exemplary points, we use a chi-squared approach. In practice, only the ATLAS Collaboration has presented the best fit values for $R^h(\gamma\gamma, ZZ \to 4\ell, WW \to \ell\nu\ell\nu)$ along with 1σ upper and lower errors as a function of m_h. Identifying h with the NMSSM h_1, we have employed Fig. 8 of [1] to compute a χ^2(ATLAS) for each point in the NMSSM parameter space (but this was not included in the global likelihood used for our MCMC scans). From Table 2 we see that the smallest χ^2(ATLAS) values (of order 0.6–0.7) are obtained for $m_{h_1} \sim 124$ GeV. This is simply because at this mass the ATLAS fits to $R^h(\gamma\gamma)$ and $R^h(4\ell)$ are very close to one, the natural prediction in the NMSSM context. For $m_h \sim 125$ GeV, the R^h's for the ATLAS data are somewhat larger than 1 leading to a discrepancy with the NMSSM SM-like prediction and a roughly doubling of χ^2(ATLAS) to values of order 1.3 to 1.6 for our exemplary points. In this context, we should note that at a Higgs mass of 125 GeV the CMS data is best fit if the Higgs signals are not enhanced and, indeed, are very close to SM values.
- The mass of the neutralino LSP, $\widetilde{\chi}_1^0$, is rather similar, $m_{\widetilde{\chi}_1^0} \approx$ 300–450 GeV, for the different perfect and almost perfect points with $m_{h_1} \gtrsim 124$ GeV. For all but pt. #5, the $\widetilde{\chi}_1^0$ is approximately an equal mixture of higgsino and bino. There is some variation in the primary annihilation mechanism, with $\widetilde{\tau}_1\widetilde{\tau}_1$ and $\widetilde{\chi}_1^0\widetilde{\chi}_1^0$ annihilation being the dominant channels except for pt. #2 for which $\widetilde{\nu}_\tau\widetilde{\nu}_\tau$ and $\widetilde{\nu}_\tau\overline{\widetilde{\nu}}_\tau$ annihilations are dominant. In the case of dominant $\widetilde{\tau}_1\widetilde{\tau}_1$ annihilation, the bulk of the $\widetilde{\chi}_1^0$'s come from those $\widetilde{\tau}$'s that have not annihilated against one another or co-annihilated with a $\widetilde{\chi}_1^0$.
- All the tabulated points yield a spin-independent direct detection cross section of order $(3.5\text{–}6) \times 10^{-8}$ pb. For the above $m_{\widetilde{\chi}_1^0}$ values, current limits on $\sigma_{\rm SI}$ are not that far above this mark and upcoming probes of $\sigma_{\rm SI}$ will definitely reach this level.
- The 7 points all have $m_{\tilde{g}}$ and $m_{\tilde{q}}$ above 1.5 TeV and in some cases above 2 TeV. Detection of the superparticles may have to await the LHC upgrade to 14 TeV.
- Only the $\tilde{t}_1$ is seen to have a mass distinctly below 1 TeV for the tabulated points. Still, for all the points $m_{\tilde{t}_1}$ is substantial, ranging from ~ 500 GeV to above 1 TeV. For such masses, detection of the $\tilde{t}_1$ as an entity separate from the other squarks and the gluino will be quite difficult and again may require the 14 TeV LHC upgrade.
- The effective superpotential μ-term, $\mu_{\rm eff}$, is small for all the exemplary points. This is interesting regarding the question of electroweak fine-tuning.

For completeness, we have run separate scans for the case of the cNMSSM of [14,15] with completely universal $m_0 = 0$ and $A_0 \equiv A_t = A_b = A_\tau = A_\lambda = A_\kappa$ (which is in fact a limit case of our model **III**). Here, one can have a singlino LSP. This requires small $\lambda < 10^{-2}$. Correct relic density is achieved via co-annihilation with $\tilde{\tau}_R$ for the rather definite choice of $A_0 \sim -\frac{1}{4}M_{1/2}$. For small enough $m_{1/2}$, the h_1 is dominantly singlet, while the h_2 is SM-like. For larger $m_{1/2}$, the h_1 is SM-like, and the h_2 is mostly singlet. The cross-over where h_1 and h_2 are highly mixed occurs roughly in the range of $m_{1/2} = 500\text{–}600$ GeV, depending on λ. Overall, we find that the h_1 can attain a mass of at most ~ 121 GeV in this scenario in the limit of large $m_{1/2}$.[3] The h_2, on the other hand, can have a mass in the 123–128 GeV range for not too large $m_{1/2}$. For $\lambda = 10^{-2}$, this happens in the region of the cross-over where $R^{h_2}(\gamma\gamma)$ is of order 0.5–0.6. Squark and gluino masses are around 1.2–1.3 TeV in this case, and hence highly pressed by LHC exclusion

[3] A similar conclusion was reached in [4] based on a mSUGRA scenario with $m_0 \approx 0$ and $A_0 \approx -\frac{1}{4}M_{1/2}$, which approximately corresponds to the cNMSSM case with the singlet Higgs superfield decoupling from the rest of the spectrum; a maximum h^0 mass of 123.5 GeV was found in this case.

Table 1
Input parameters for the exemplary points. We give $\tan\beta(m_Z)$ and GUT scale parameters, with masses in GeV and masses-squared in GeV^2. Starred points are the perfect points satisfying all constraints, including $\delta a_\mu > 5.77\times10^{-10}$ and $0.094 < \Omega h^2 < 0.136$. Unstarred points are the almost perfect points that have $4.27\times10^{-10} < \delta a_\mu < 5.77\times10^{-10}$ and $0.094 < \Omega h^2 < 0.136$.

Pt. #	Model II			Model III			
	1*	2*	3	4*	5	6	7
$\tan\beta(m_Z)$	17.9	17.8	21.4	15.1	26.2	17.9	24.2
λ	0.078	0.0096	0.023	0.084	0.028	0.027	0.064
κ	0.079	0.011	0.037	0.158	−0.045	0.020	0.343
$m_{1/2}$	923	1026	1087	842	738	1104	1143
m_0	447	297	809	244	1038	252	582
A_0	−1948	−2236	−2399	−1755	−2447	−2403	−2306
A_λ	0	0	0	−251	−385	−86.8	−2910
A_κ	0	0	0	−920	883	−199	−5292
$m^2_{H_d}$	$(2942)^2$	$(3365)^2$	$(4361)^2$	$(2481)^2$	$(935)^2$	$(3202)^2$	$(3253)^2$
$m^2_{H_u}$	$(1774)^2$	$(1922)^2$	$(2089)^2$	$(1612)^2$	$(1998)^2$	$(2073)^2$	$(2127)^2$

Table 2
Upper section: Higgs masses. Middle section: reduced h_1 couplings to up- and down-type quarks, $V = W, Z$ bosons, photons, and gluons. Bottom section: total width in GeV, decay branching ratios, $R^{h_1}(\gamma\gamma)$, $R^{h_1}(VV)$ and $\chi^2_{\rm ATLAS}$ of the lightest CP-even Higgs for the seven exemplary points.

Pt. #	Model II			Model III			
	1*	2*	3	4*	5	6	7
m_{h_1}	124.0	125.1	125.4	123.8	124.5	125.2	125.1
m_{h_2}	797	1011	1514	1089	430	663	302
m_{a_1}	66.5	9.83	3.07	1317	430	352	302
C_u	0.999	0.999	0.999	0.999	0.999	0.999	0.999
C_d	1.002	1.002	1.001	1.003	1.139	1.002	1.002
C_V	0.999	0.999	0.999	0.999	0.999	0.999	0.999
$C_{\gamma\gamma}$	1.003	1.004	1.004	1.004	1.012	1.003	1.001
C_{gg}	0.987	0.982	0.988	0.984	0.950	0.986	0.994
$\Gamma_{\rm tot}(h_1)$ [GeV]	0.0037	0.0039	0.0039	0.0037	0.0046	0.0039	0.0039
BR($h_1\to\gamma\gamma$)	0.0024	0.0024	0.0024	0.0024	0.002	0.0024	0.0024
BR($h_1\to gg$)	0.056	0.055	0.056	0.056	0.043	0.055	0.056
BR($h_1\to b\bar{b}$)	0.638	0.622	0.616	0.643	0.680	0.619	0.621
BR($h_1\to WW$)	0.184	0.201	0.207	0.180	0.159	0.203	0.201
BR($h_1\to ZZ$)	0.0195	0.022	0.023	0.019	0.017	0.022	0.022
$R^{h_1}(\gamma\gamma)$	0.977	0.970	0.980	0.980	0.971	0.768	0.975
$R^{h_1}(ZZ, WW)$	0.971	0.962	0.974	0.974	0.964	0.750	0.969
$\chi^2_{\rm ATLAS}$	0.59	1.27	1.47	0.72	1.57	1.34	1.20

Table 3
Top section: $\mu_{\rm eff}$ and sparticle masses at the SUSY scale in GeV. Bottom section: LSP decomposition. $m_{\tilde{q}}$ is the average squark mass of the first two generations. The LSP bino, wino, higgsino and singlino fractions are $f_{\tilde{B}} = N^2_{11}$, $f_{\tilde{W}} = N^2_{12}$, $f_{\tilde{H}} = N^2_{13} + N^2_{14}$ and $f_{\tilde{S}} = N^2_{15}$, respectively, with N the neutralino mixing matrix.

Pt. #	Model II			Model III			
	1*	2*	3	4*	5	6	7
$\mu_{\rm eff}$	400	447	472	368	421	472	477
$m_{\tilde{g}}$	2048	2253	2397	1876	1699	2410	2497
$m_{\tilde{q}}$	1867	2020	2252	1685	1797	2151	2280
$m_{\tilde{b}_1}$	1462	1563	1715	1335	1217	1664	1754
$m_{\tilde{t}_1}$	727	691	775	658	498	784	1018
$m_{\tilde{e}_L}$	648	581	878	520	1716	653	856
$m_{\tilde{e}_R}$	771	785	1244	581	997	727	905
$m_{\tilde{\tau}_1}$	535	416	642	433	784	443	458
$m_{\widetilde{\chi}^\pm_1}$	398	446	472	364	408	471	478
$m_{\widetilde{\chi}^0_1}$	363	410	438	328	307	440	452
$f_{\tilde{B}}$	0.506	0.534	0.511	0.529	0.914	0.464	0.370
$f_{\tilde{W}}$	0.011	0.009	0.008	0.012	0.002	0.009	0.009
$f_{\tilde{H}}$	0.483	0.457	0.482	0.459	0.083	0.528	0.622
$f_{\tilde{S}}$	10^{-4}	10^{-6}	10^{-6}	10^{-4}	10^{-6}	10^{-4}	10^{-6}

limits. For smaller λ, an h_2 with mass near 125 GeV is always singlet-like and its signal strength in the $\gamma\gamma$ and VV channels is very much suppressed relative to the prediction for the SM Higgs, in apparent contradiction to the ATLAS and CMS results.

In summary, we find that the fully constrained version of the NMSSM is not able to yield a Higgs boson consistent with the current hints from LHC data for a fairly SM-like Higgs with mass ~ 125 GeV, once all experimental constraints are imposed including acceptable a_μ and Ωh^2 in the WMAP window. However, by relaxing the CNMSSM to allow for non-universal Higgs soft-masses-squared (NUHM scenarios), it is possible to obtain quite perfect points in parameter space satisfying all constraints with

Table 4
δa_μ in units of 10^{-10}, LSP relic abundance, primary annihilation channels and spin-independent LSP scattering cross section off protons.

Pt. #	δa_μ	Ωh^2	Prim. Ann. Channels	$\sigma_{\rm SI}$ [pb]
1*	6.01	0.094	$\widetilde{\chi}_1^0\widetilde{\chi}_1^0 \to W^+W^-$(31.5%), ZZ(21.1%)	4.3×10^{-8}
2*	5.85	0.099	$\widetilde{\nu}_\tau\widetilde{\nu}_\tau \to \nu_\tau\nu_\tau$(11.4%), $\widetilde{\nu}_\tau\widetilde{\nu}_\tau \to W^+W^-$(8.8%)	3.8×10^{-8}
3	4.48	0.114	$\widetilde{\chi}_1^0\widetilde{\chi}_1^0 \to W^+W^-$(23.9%), ZZ(17.1%)	3.7×10^{-8}
4*	6.87	0.097	$\widetilde{\chi}_1^0\widetilde{\chi}_1^0 \to W^+W^-$(36.9%), ZZ(23.5%)	4.5×10^{-8}
5	5.31	0.135	$\widetilde{\chi}_1^0\widetilde{\chi}_1^0 \to b\bar{b}$(39.5%), h_1a_1(20.3%)	5.8×10^{-8}
6	4.89	0.128	$\widetilde{\tau}_1\widetilde{\tau}_1 \to \tau\tau$(17.4%), $\widetilde{\chi}_1^0\widetilde{\chi}_1^0 \to W^+W^-$(14.8%)	4.0×10^{-8}
7	4.96	0.101	$\widetilde{\chi}_1^0\widetilde{\chi}_1^0 \to W^+W^-$(17.7%), ZZ(12.9%)	4.0×10^{-8}

$m_{h_1} \sim 125$ GeV even if the attractive $U(1)_R$ symmetry limit of $A_\lambda = A_\kappa = 0$ is imposed at the GUT scale and certainly if general A_λ and A_κ values are allowed. We observe a mild tension between the a_μ constraint and obtaining $m_{h_1} \sim 125$ GeV; just slightly relaxing the a_μ requirement makes it much easier to find viable points with $m_{h_1} \sim 125$ GeV, thus opening up interesting regions of parameter space. We also note that our scanning suggests that relatively small A_λ, A_κ values are preferred for (almost) perfect points. Masses of SUSY particles for perfect/almost perfect points are such that direct detection of SUSY may have to await the 14 TeV upgrade of the LHC. However, the predicted $\widetilde{\chi}_1^0$ masses and associated spin-independent cross sections suggest that direct detection of the $\widetilde{\chi}_1^0$ will be possible with the next round of upgrades to the direct detection experiments.

Acknowledgements

We would like to thank Sezen Sekmen for helpful contributions regarding the MCMC program structure. This work has been supported in part by US DOE grant DE-FG03-91ER40674 and by IN2P3 under contract PICS FR–USA No. 5872.

References

[1] ATLAS Collaboration, Combination of Higgs boson searches with up to 4.9 fb^{-1} of pp collisions data taken at a center-of-mass energy of 7 TeV with the ATLAS experiment at the LHC, ATLAS-CONF-2011-163.
[2] CMS Collaboration, Combination of SM Higgs searches, CMS-PAS-HIG-11-032.
[3] H. Baer, V. Barger, A. Mustafayev, Implications of a 125 GeV Higgs scalar for LHC SUSY and neutralino dark matter searches, arXiv:1112.3017.
[4] A. Arbey, M. Battaglia, A. Djouadi, F. Mahmoudi, J. Quevillon, Implications of a 125 GeV Higgs for supersymmetric models, arXiv:1112.3028.
[5] A. Arbey, M. Battaglia, F. Mahmoudi, Constraints on the MSSM from the Higgs sector — A pMSSM study of Higgs searches, $B_s \to \mu^+\mu^-$ and dark matter direct detection, arXiv:1112.3032.
[6] M. Carena, S. Gori, N.R. Shah, C.E. Wagner, A 125 GeV SM-like Higgs in the MSSM and the $\gamma\gamma$ rate, arXiv:1112.3336.
[7] O. Buchmueller, R. Cavanaugh, A. De Roeck, et al., Higgs and supersymmetry, arXiv:1112.3564 [hep-ph].
[8] S. Akula, B. Altunkaynak, D. Feldman, P. Nath, G. Peim, Higgs boson mass predictions in SUGRA unification, recent LHC-7 results, and dark matter, arXiv:1112.3645.
[9] M. Kadastik, K. Kannike, A. Racioppi, M. Raidal, Implications of 125 GeV Higgs boson on scalar dark matter and on the CMSSM phenomenology, arXiv:1112.3647.
[10] J. Cao, Z. Heng, D. Li, J.M. Yang, Current experimental constraints on the lightest Higgs boson mass in the constrained MSSM, arXiv:1112.4391.
[11] A. Arvanitaki, G. Villadoro, A non-Standard Model Higgs at the LHC as a sign of naturalness, arXiv:1112.4835.
[12] L.J. Hall, D. Pinner, J.T. Ruderman, A natural SUSY Higgs near 126 GeV, arXiv:1112.2703.
[13] U. Ellwanger, A Higgs boson near 125 GeV with enhanced di-photon signal in the NMSSM, arXiv:1112.3548.
[14] A. Djouadi, U. Ellwanger, A.M. Teixeira, Phys. Rev. Lett. 101 (2008) 101802, arXiv:0803.0253.
[15] A. Djouadi, U. Ellwanger, A.M. Teixeira, JHEP 0904 (2009) 031, arXiv:0811.2699.
[16] U. Ellwanger, J.F. Gunion, C. Hugonie, JHEP 0502 (2005) 066, arXiv:hep-ph/0406215.
[17] U. Ellwanger, C. Hugonie, Comput. Phys. Commun. 175 (2006) 290, arXiv:hep-ph/0508022.
[18] http://www.th.u-psud.fr/NMHDECAY/nmssmtools.html.
[19] A. Djouadi, J. Kalinowski, M. Spira, Comput. Phys. Commun. 108 (1998) 56, arXiv:hep-ph/9704448.
[20] R. Dermisek, J.F. Gunion, Phys. Rev. D 75 (2007) 075019, arXiv:hep-ph/0611142.
[21] B.A. Dobrescu, K.T. Matchev, JHEP 0009 (2000) 031, arXiv:hep-ph/0008192.